Observation of a Dynamic Wetting Process Using Laser-Doppler Velocimetry

The purpose of this study is to observe the dynamic wetting process of a slide coater flow ($Ca = 0.16$; $Re = 14.4$; $St = 0.0142$; $\Delta eP = 2.5$), using a specially-developed Laser-Doppler measuring technique.

The measurements, carried out with glycerol solutions, reveal that the observed contact line is apparent and that a thin air film is entrained between the web and the liquid surface. The liquid is accelerated along the lower free surface and attains approximately 50% of the web velocity at the apparent contact line. Downstream from the apparent contact line, the liquid is further accelerated along the air film to the web velocity at the real contact line.

The apparent contact angle increases with the capillary number Ca and air entrainment occurs at $Ca = 0.25$.

W. Mues
J. Hens
L. Boiy
Res. Labs.
Agfa-Gevaert N.V.
Mortsel, Belgium

Introduction

Despite considerable efforts, the dynamic wetting process of a moving solid surface by a liquid is still poorly understood. Research in this area faces three major difficulties:

- The wetting process involves both hydrodynamic and molecular forces.
- The wetting phenomena take place on a very small scale, almost inaccessible to observation.
- Wetting is not a static, but a dynamic, process.

Hence, observation of what really happens is very difficult. After many years of investigations, there still is no agreement among researchers whether an observed contact angle is apparent or real (Ngan and Dussan, 1982).

The literature on wetting is very extensive, and only a few main topics will be addressed in this survey. Huh and Scriven (1971), and Dussan and Davis (1974) pointed out that the hydrodynamic no-slip condition combined with contact angles being smaller than 180° must lead to physical singularities, which can be removed only by *ad-hoc* hypotheses, such as slippage models (Huh and Mason, 1977). Dussan and Davis (1974) suggested a rolling motion of the liquid.

Pismen and Nir (1982) calculated the flow geometry in the vicinity of the contact line at very low capillary numbers and came to the conclusion that the liquid-air interface curves continuously until it becomes tangent to the solid surface at the contact line.

Burley and Kennedy (1976), Rillaerts and Joos (1980), and Gutoff and Kendrick (1982) experimentally derived relationships between the critical velocity and the main influencing parameters. Although this kind of approach has its practical usefulness, it does not shed any light at the underlying physical wetting mechanisms.

Deryagin and Levi (1964) first assumed that a thin air film is being entrained between the web and the liquid surface. This assumption was developed by Miyamoto and Scriven (1982), who investigated the conditions at which this air film collapses. Miyamoto (1986) showed that in a coated layer small amounts of air are trapped at subcritical velocities.

In summary, more evidence is needed to support some of the interesting hypotheses, which have been put forward in the literature.

A Laser-Doppler velocimetry setup, featuring a very small measuring volume, was used for measurements close to the moving contact line in a slide coater bead. The measurements, carried out with glycerol solutions, yielded the velocity distribution in the liquid and the geometry of the free liquid surface in the immediate vicinity of the observed contact line.

Downstream from the observed contact line, a thin air film is entrained between the web and the liquid, which confirms the hypothesis of Miyamoto and Scriven (1982). Consequently, the observed contact line is an apparent one. The liquid velocity increases along the free liquid surface towards the observed contact line, where it amounts to 40 to 60% of the web velocity, which is attained at the real contact line, located between 50 and 125 μm downstream from the observed contact line.

Correspondence concerning this paper should be addressed to J. Hens.

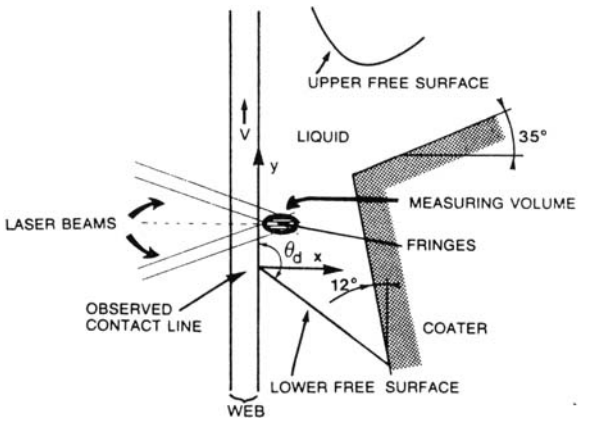

Figure 1. Experimental setup.

In the vicinity of the contact line, the liquid is subjected to extremely high accelerations and shear rates, which may affect its rheological behavior.

Experimental Setup

The purpose of the experimental setup is to measure liquid velocities in a slide coater bead (Figure 1), bounded by the vertically moving web, which is a subbed polyester film, the front face of the coater, the upper and the lower free surface, without disturbing the flow and to determine the location of the lower free surface.

The only method available is Laser-Doppler Velocimetry. The main features of the optical arrangement used have been described in the literature (Oldengarm et al., 1975). A 10-mW HeNe-laser beam (Figure 2) is focused by a lens L 1 on a rotating grating, which splits the beam into one zero-order beam and pairs of higher-order beams. Only the two first-order beams, forming an angle of 12° with one another, are used. The diffraction grating has 16,384 pairs of lines on its circumference and rotates at 50 rev./s. The rotating grating provides a bias frequency upon which the frequency generated by the moving particles in the liquid is superposed. This permits the determination of the flow direction. The two beams are focused through lenses L 2 and L 3 and form an interference pattern at their intersection, where they build the measuring volume. The beams intersect in the liquid bead (Figure 1) after passing through the web. The liquid is seeded with silicium carbide particles, which scatter the beams.

The signal generated by the particles moving through the measuring volume consists of the sum of two frequencies: 1. the bias frequency, and 2. the Doppler frequency ν_D, which can be calculated by the following relation:

$$\nu_D = \frac{2v_y \sin \varphi/2}{\lambda}$$

where λ is the wavelength of the laser light (632.8×10^{-9} m); φ is the angle between the two beams ($\varphi = 45°$); and v_y is the liquid velocity component perpendicular to the fringes.

The light reflected by the particles in the liquid is captured by mirror M 1 and sent over mirror M 2 to a photomultiplier, which feeds the electronic signals to a frequency tracker. As the liquid velocity can vary over the width of the measuring volume, the signal contains a spectrum of frequencies. The tracker selects the frequency with the highest intensity and calculates its velocity. Because the light intensity in the measuring volume has a Gaussian distribution and its maximum is located at the center of the measuring volume, the tracker generally selects the velocity signal corresponding with the liquid velocity in the center of the measuring volume.

As the bead of a slide coater is very small, we aimed at minimizing the dimensions of the measuring volume. It can be proved (Oldengarm et al., 1975) that the length b_x of the measuring volume on the optical axis is:

$$b_x = \frac{4n\lambda f_1 f_3}{\pi f_2 b_0 \sin \varphi/2}$$

where n is the refractive index of the liquid; f_i is the focal length of lens i; and b_0 is the diameter of the laser beam. This relation shows that a small b_x value can be obtained by choosing small values for f_1 and f_3, and large values for f_2 and φ. With $f_1 = 20$ mm, $f_2 = 200$ mm, $f_3 = 50$ mm, $b_0 = 1$ mm, $\lambda = 632.8 \times 10^{-9}$ m, $\varphi = 45°$, and $n = 1.45$ (glycerol solution):

$$b_x = 15.26\ \mu\text{m}.$$

In practice, in order to get the smallest measuring volume possible, much care must be taken over the alignment of the optics. The laser beams must cross each other at their waists; otherwise, b_x is not minimal and the fringes are not planparallel. Due to imperfections of the lenses, the smallest obtainable b_x value is much larger than the theoretical one and is about 40 μm. It must be emphasized, however, that generally the signal issuing from the center of the measuring volume is selected by the tracker and recorded. Hence, the resolution of the measurements is much better than 40 μm.

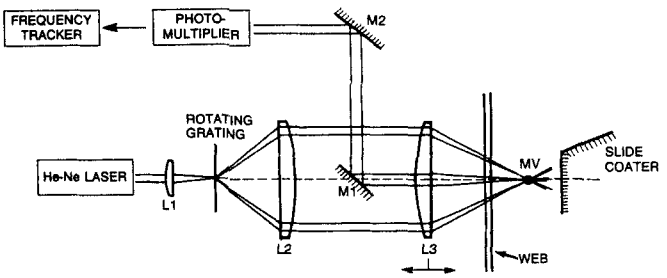

Figure 2. Optical arrangement.

Laser-Doppler Measurements in a Slide-Coater Bead

A slide coater bead, characterized by the following dimensionless numbers, was investigated:

Capillary number *Ca:*

$$\mu V/\sigma = 0.16$$

Reynolds number *Re:*

$$\rho VL/\mu = 14.4$$

Stokes number St:

$$\rho L^2 g/\mu V = 0.0142$$

Dimensionless vacuum number ΔeP:

$$\Delta pL/\mu V = 2.5$$

where L is the eventual layer thickness ($L = 100$ μm); V, the web velocity ($V = 1$ m/s); μ, the liquid viscosity ($\mu = 8.10^{-3}$ Pa · s); ρ, the liquid density ($\rho = 1{,}155$ kg/m^3); σ, the surface tension of the liquid ($\sigma = 50.10^{-3}$ N/m); Δp the vacuum beneath the bead ($\Delta p = 200$ Pa).

By shifting L 3 along the optical axis, the measuring volume is moved in the bead between the web and the front face of the coater, and a continuous liquid velocity profile is obtained. Successively three velocity profiles are recorded at y levels of 200 μm and 50 μm, respectively, downstream from the observed contact line and 50 μm beneath the observed contact line.

Velocity Profile: 200 μm Downstream from Observed Contact Line

Figure 3 shows the velocity profile obtained 200 μm downstream from the observed contact line. The velocity profile corresponds to the profile expected in a closed system: the total flow rate, represented by the area between abcissa and velocity curve, is zero. The slope of the velocity graph represents the shear rate, which amounts to 1.5×10^{-4} s^{-1} at the web. At smaller y values (closer to the observed contact line), the shear rates are much higher.

Velocity Profile: 50 μm Downstream from Observed Contact Line

The velocity profile displayed in Figure 4 exhibits some unexpected features. A velocity plateau AB, at web velocity, followed by a steep drop BC, is noticed. From C to D, the velocity drops gradually. At D it starts to rise unexpectedly, until it reaches E where it starts to drop normally. When velocity profiles are recorded closer to the observed contact line, the velocity jump BC grows larger and the discontinuity at D occurs at smaller x values.

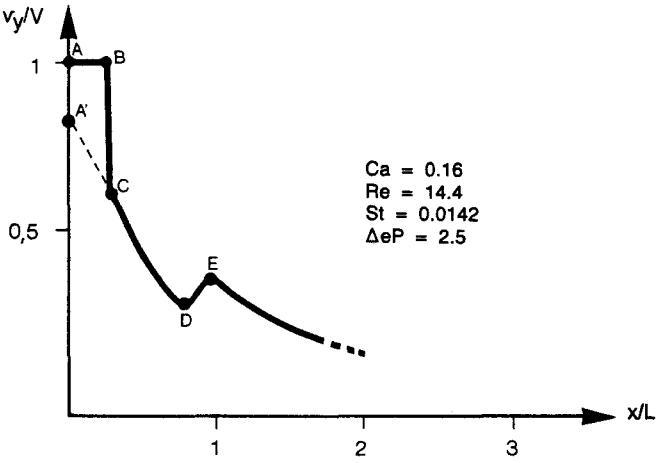

Figure 4. Velocity profile 50 μm downstream from the observed contact line.

The velocity plateau AB can be explained by the assumption of a thin air film being entrained between web and liquid. Due to large differences in refractive indices of the polyethylene terephthalate web ($n_w = 1.5$) and air ($n_a = 1$), a significant part of the laser light is reflected at the web-air interface (Figure 5) and forms a new measuring volume 2 in the web. The tracker selects the signal emitted by measuring volume 2, because it is stronger than the signal emitted by measuring volume 1. Hence, the recorded velocity is the web velocity. It should be emphasized that the width of the plateau AB is independent of the air film thickness. As soon as the distance of the measuring volume 1 to the web exceeds AB, its signal supersedes the signal from measuring volume 2.

The same result is obtained without liquid between web and coater, which confirms the assumption that the velocity plateau AB is caused by an air film between the web and the liquid.

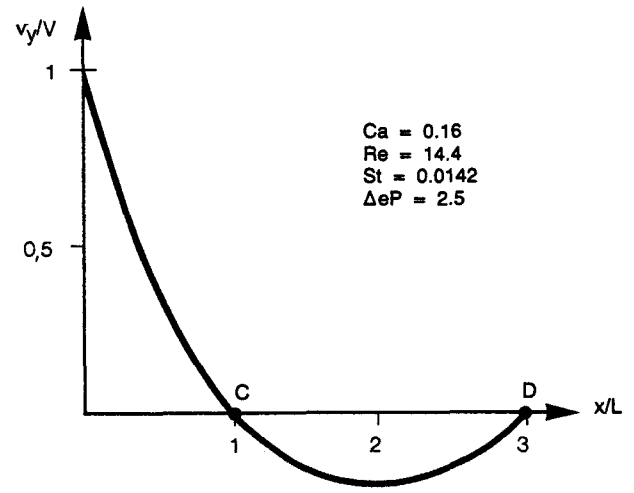

Figure 3. Velocity profile 200 μm downstream from the observed contact line.

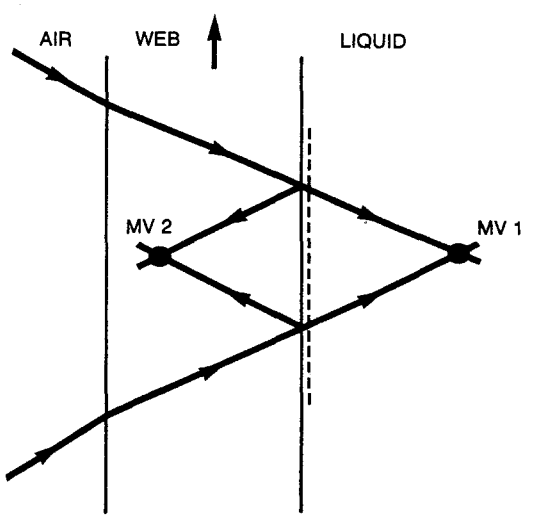

Figure 5. Formation of measuring volume 2 by reflecting laser beams at the web-liquid interface.

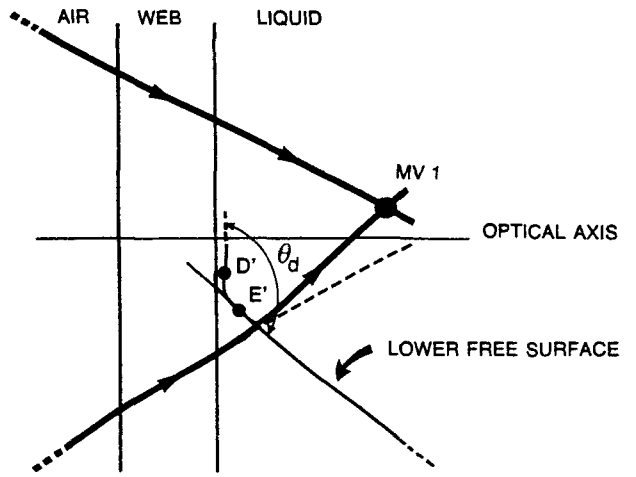

Figure 6. Shifting of measuring volume 1 by deflecting laser beams at the lower free surface.

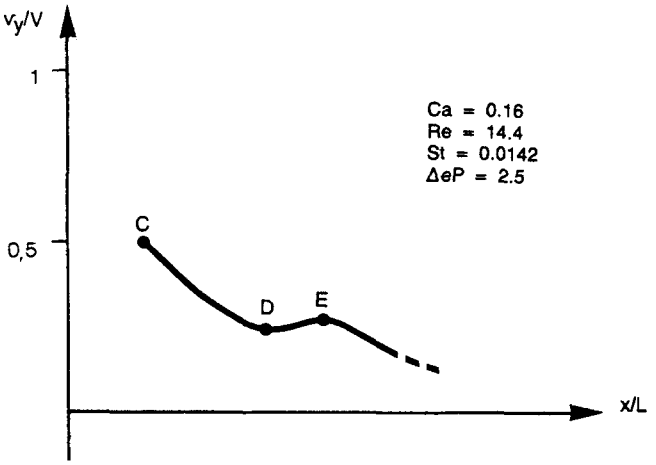

Figure 7. Velocity profile 50 μm beneath the observed contact line.

The disturbing velocity signal can be filtered electronically. When moving measuring volume 1 from right to left, the dotted line on Figure 4 is obtained. The liquid velocity at the liquid-air interface in A' is smaller than the web velocity. The velocity difference $(V - V_{A'})$ continuously decreases when measuring at increasing y values. The real contact line is located at about 105 μm downstream from the observed contact line, where $(V - V_{A'})$ becomes zero.

Figure 6 shows that, when the lower laser beam leaves the web beneath the observed contact line, it is deflected by the air-liquid interface at the lower free surface of the bead, which forms an angle Θ_d with the web. Hence, measuring volume 1 is no more located on the optical axis, but somewhere above. The observed contact line is actually the intersection of the extension of the lower free surface and the web. Close to the web, the free surface bends sharply ($D'E'$). The velocity shift DE (Figure 4) is due to the deflection of the lower laser beam at $D'E'$ and the ensuing shifting of measuring volume 1 above the optical axis. The value $(x_E - x_D)$ is related to the radius of curvature at the interface $D'E'$ in the vicinity of the contact line.

Velocity Profile 50 μm Beneath Observed Contact Line

The velocity profile shown on Figure 7 exhibits features similar to the features of the profile shown in Figure 4. Here the disturbing signal has likewise been eliminated by filtering. The location and the velocity component v_y of the lower free surface can be derived from the measurements. As in the previous case, a discontinuity in the location of the measuring volume arises between D and E. In this case, it is caused by the deflection of the upper laser beam as soon as it leaves the web above the observed contact line.

Another important feature of the Laser-Doppler Velocimeter measurements is that they allow the observed contact line to be located accurately. Figure 8 shows the location of D and E for different y values of the optical axis, above and beneath the observed contact line. It can easily be proved by geometrical considerations, and it has been confirmed experimentally that straight lines can be drawn through the D's and E's. These straight lines converge accurately at the observed contact line.

Evaluation of Results

The Laser-Doppler Velocimeter measurements allow the following conclusions to be drawn:

1. Downstream from the observed contact line, a thin, invisible air film is entrained between web and liquid, which confirms the hypothesis of Miyamoto and Scriven (1982). In the case considered above, the length of this air film is approximately 105 μm. The real contact line is located 105 μm downstream from the observed one.

2. The observed contact line is not the real contact between liquid and web, but the intersection of the extended lower free surface of the bead and the web surface. Actually, close to the web (within 10 μm), the lower free surface bends sharply in the direction of the web surface, without getting in touch with it. The calculations of Pismen and Nir (1982) at very low capillary numbers, however, support our observations. The Laser-Doppler velocimeter measurement technique allows an accurate location of the apparent contact line.

3. The apparent contact angle Θ_d can be derived from the measurements of the location of the lower free surface at dif-

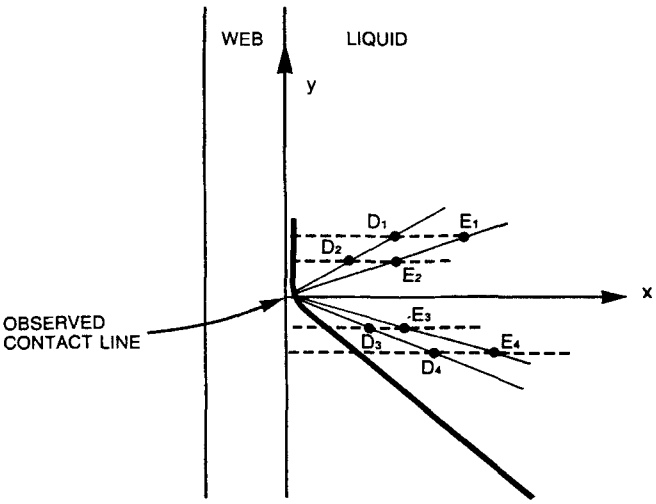

Figure 8. Locating the observed contact line by connecting D_i or E_i with straight lines.

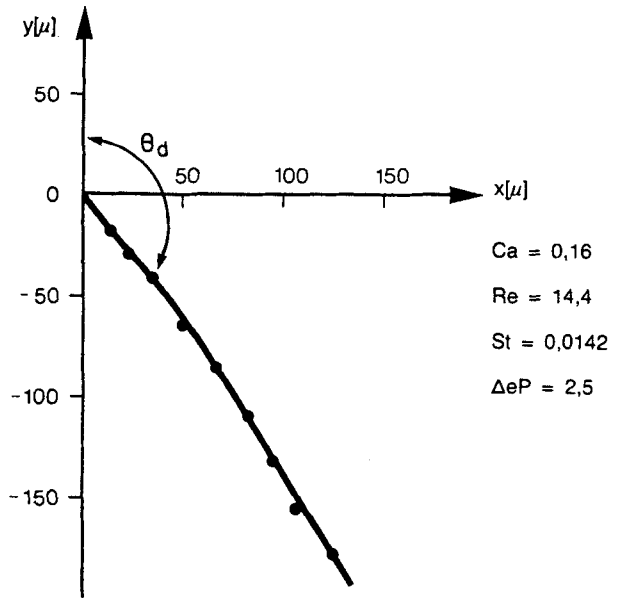

Figure 9. Location of the lower free surface and determination of Θ_D.

ferent y values (Figure 9). As the lower free surface cannot always exactly be represented by a straight line, the determination of Θ_d is not very accurate ($\pm 3°$).

4. The velocity component v_y along the lower free surface (y') increases when approaching the web (Figure 10). At the apparent contact line, v_y attains 45% of the web velocity. Downstream from the apparent contact line, the liquid is progressively accelerated along the air film until it reaches the web velocity. This acceleration is due to extensional forces. The mean acceleration between apparent and real contact lines is 4,200 m/s^2 or 428 g!

5. Although no unbounded forces or multivalued velocities are involved in the wetting process, some parameters attain very high values in the vicinity of the contact line: the curvature of the lower free surface, the shear rate web liquid, and the acceleration along the lower free surface. The rheological behavior of liquids under these extreme conditions is badly known and should be investigated.

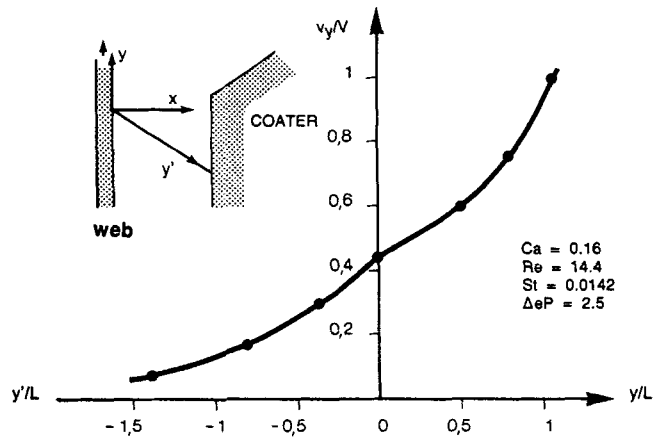

Figure 10. v_y/V along the lower free surface and the air film between web and liquid.

Table 1. Dynamic Contact Angle and Air Film Length

Ca	*Re*	*St*	*ΔeP*	Θ_d	cos Θ_d	*l*, μm
0.16	14.4	0.014	2.5	147	−0.839	105
0.106	9.6	0.021	3.75	139	−0.755	55
0.16	7.2	0.003	1.25	154	−0.899	85
0.16	21.6	0.032	3.75	146	−0.829	115
0.16	14.4	0.014	1.25	149	−0.857	120
0.16	14.4	0.014	3.75	148	−0.848	70
0.12	19.1	0.019	3.33	135	−0.707	115
0.24	9.8	0.009	1.67	149	−0.857	35
0.05	14.1	0.031	5.56	122	−0.530	—

The Laser-Doppler velocimeter measurements do not reveal all the details of the flow geometry in the vicinity of the contact line:

1. They do not allow to determine accurately the curvature of the lower free surface at the observed contact line. They only indicate that the radius of curvature is smaller than 10 μm.

2. Neither do they allow the determination of the thickness of the entrained air film nor the determination of the actual interfacial shape at the real contact line. As the interfacial shape at the real contact line is at least partly determined by molecular forces operating at a length scale of Angströms, optical methods, with a resolution of several micrometers, are unable to resolve shapes in this scale.

3. The Laser-Doppler Velocimeter measurements do not give any clue about what happens with the air being entrained between web and liquid.

Dimensionless Numbers vs. Geometry of Lower Free Surface

A series of Laser-Doppler Velocimeter measurements were carried out, whereby the dimensional variables V, L, Δp, μ, and σ were modified over following ranges:

V from 0.67 to 1 m/s
L from 50 to 150.10^{-6} m
Δp from 100 to 300 Pa
μ from 5.4 to 12.10^{-3} Pa · s
σ from 50 to 72.10^{-3} N/m

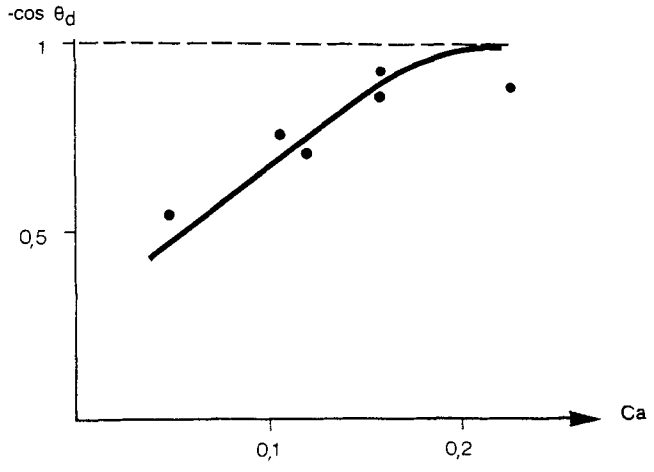

Figure 11. − cos Θ_D as a function of *Ca*.
Air entrainment occurs at $Ca = 0.25$

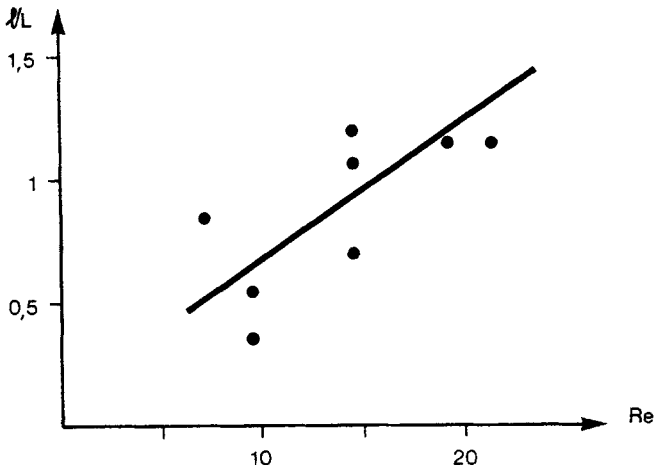

Figure 12. Dependence of l/L on *Re*.

The corresponding ranges of the dimensionless numbers were:

Ca from 0.051 to 0.24
Re from 7.2 to 21.6
St from 0.0035 to 0.032
ΔeP from 1.25 to 5.56

Table 1 gives the values of *Ca*, *Re*, *St* and ΔeP, and of the ensuing dynamic contact angle Θ_d and length l of the air film between web and liquid. Relationships between one of the dimensionless numbers and Θ_D or l were sought. Only the relationships between $\cos \Theta_D$ and *Ca* (Figure 11) and l and *Re* (Figure 12) seem meaningful.

The contact angle increases as *Ca* increases, which was to be expected. It was noticed, however, that when the contact angle exceeds 150°, the limit of coatability is rapidly attained; the coating becomes unstable. Moreover, the geometry of the lower free surface is modified (Figure 13): the radius of curvature in the vicinity of the observed contact line becomes much greater

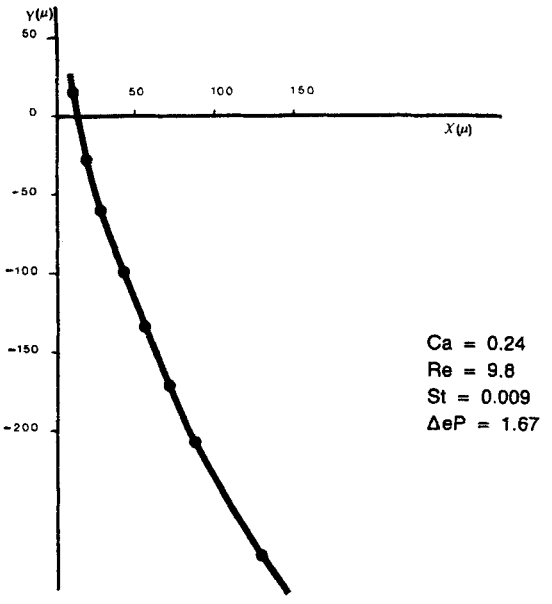

Figure 13. Location of the lower free surface with *Ca* = 0.24.

and the observed contact line can no more be located accurately. Contact angles ranging from 155° and 180° could not be observed. According to Figure 11, air entrainment ($\Theta_D = 180°$) occurs at a *Ca* value of 0.25.

The length of the air film between the observed and the real contact line increases with increasing *Re*. This can reasonably be expected as lower viscosities or higher web velocities require a greater length for the liquid to be accelerated up to the web velocity. The nature of the relationship, however, is obscured by the scattering of the points.

Acknowledgment

We are indebted to H. Geerts for his skillful technical assistance.

Notation

b_0 = diameter of the laser beam, m
b_x = projection of measuring volume on the x axis, m
Ca = capillary number
f_i = focal length of lens i, m
g = acceleration of gravity, m/s^2
l = length of the air film between web and liquid, m
L = eventual layer thickness, m
n = refractive index
Re = Reynolds number
St = Stokes number
V = web velocity, m/s
v_y = velocity in the y direction, m/s
x = axis perpendicular to the web surface
y = axis parallel to the web surface

Greek letters

Δp = vacuum beneath the liquid bead, Pa
ΔeP = dimensionless vacuum
Θ_D = dynamic contact angle, °
λ = wavelength of the laser light, m
μ = viscosity of the liquid, Pa s
ν_D = Doppler frequency, s^{-1}
ρ = density of the liquid, kg/m^3
σ = surface tension of the liquid, N/m
φ = angle between the two beams forming the measuring volume, °

Literature Cited

Burley, R., and B. S. Kennedy, "A Study of the Dynamic Wetting Behaviour of Polyester Tapes," *Br. Polym. J.*, **8**,140 (1976).
Deryagin, B. M., and S. M. Levi, *Film Coating Theory*, 143, Focal Press, London and New York (1964).
Dussan, E. B., and G. H. Davis, "On the motion of a Fluid-Fluid Interface along a Solid Surface," *J. Fluid Mech.*, **65**(1), 71 (1974).
Gutoff, E. B., and C. E. Kendrick, "Dynamic Contact Angles," *AIChE J.*, **28**(3), 459 (1982).
Huh, C., and L. E. Scriven, "Hydrodynamic Model of Steady Movement of a Solid/Liquid/Fluid Contact Line," *J. Colloid Interf. Sci.*, **35**(1), 85 (1971).
Huh, C., and S. G. Mason, "The Steady Movement of a Liquid Meniscus in a Capillary Tube," *J. Fluid Mech.*, **81**(3), 401 (1977).
Miyamoto, K., and L. E. Scriven, "Breakdown of Air Film Entrained by Liquid Coated on Web," AIChE Meeting, Los Angeles, #101g (1982).
Miyamoto, K., "On the Nature of Entrained Air Bubbles in Coating," *AIChE Symp. Mech. Thin-Film Coating*, New Orleans, #86c (1986).
Ngan, C. G., and E. B. Dussan, "On the Nature of the Dynamic Contact Angle: An Experimental Study," *J. Fluid Mech.*, **118**, 27 (1982).
Oldengarm, J., A. H. van Krieken, and H. W. Van der Klooster, "Velocity Profile Measurements in a Liquid Film Flow Using the Laser Doppler Technique," *J. of Phys.* **8**, 203 (1975).
Pismen, L. M., and A. Nir, "Motion of a Contact Line," *Phys. Fluids*, **25**(1), 3 (1982).
Rillaerts, E., and P. Joos, "The Dynamic Contact Angle," *Chem. Eng. Sci.*, **35**, 883 (1980).

Manuscript received Jan. 3, 1989, and revision received June 14, 1989.